THE JOURNAL OF PHYSICAL CHEMISTRY B

Comment

pubs.acs.org/JPCB

Reply to "Comment on 'Proton Transfer of Guanine Radical Cations Studied by Time-Resolved Resonance Raman Spectroscopy Combined with Pulse Radiolysis'"

Jungkweon Choi,[*,†,‡] Cheolhee Yang,[‡,§] Mamoru Fujitsuka,[†] Sachiko Tojo,[†] Hyotcherl Ihee,[‡,§] and Tetsuro Majima[*,†]

[†]The Institute of Scientific and Industrial Research (SANKEN), Osaka University, Mihogaoka 8-1, Ibaraki, Osaka 567-0047, Japan

[‡]Center for Nanomaterials and Chemical Reactions, Institute for Basic Science (IBS), Daejeon 305-701, Republic of Korea

[§]Department of Chemistry, Korea Advanced Institute of Science and Technology (KAIST), Daejeon 305-701, Republic of Korea

J. Phys. Chem. B **2016**, *120*. DOI: 10.1021/acs.jpcb.5b12607

We recently reported proton transfer of guanine (G) radical cation ($G^{\bullet+}$) formed by one-electron oxidation using transient absorption and time-resolved resonance Raman (TR^3) spectroscopies combined with pulse radiolysis.[1] In our previous study, we suggested that the neutral radical of G ($G^{\bullet}(-H^+)$), generated by the deprotonation of G radical cation ($G^{\bullet+}$), is rapidly converted to a new G radical species, $(G^{\bullet+})'$, formed from the protonation at the N7. On one hand, the Raman spectrum of $(G^{\bullet+})'$ shows the characteristic C6−O stretching mode at ∼1266 cm^{-1} corresponding to a C6−O single bond, which indicates that the unpaired electron in $(G^{\bullet+})'$ is localized on the oxygen of the pyrimidine (Pyr) ring. However, on the basis of the results of quantum chemical calculations, Sevilla et al. challenge one of the interpretations of our results.

Quantum chemical calculations by Sevilla et al. demonstrated that all G radical species as well as 5′-dGMP showed the C6═O stretching at >1600 cm^{-1}, 1716 cm^{-1} for 5′-dGMP, 1747 cm^{-1} for $G^{\bullet+}$, 1668 cm^{-1} for $(G^{\bullet+})'$, and 1608−1654 cm^{-1} for $G^{\bullet}(-H^+)$. On the basis of their results of density functional theory (DFT) calculations, all G radical species have a C═O double bond character and the unpaired electron is fully delocalized. Consequently, they concluded that our interpretation for the localization of the unpaired electron at O6 and the reprotonation at N7 is in error.

To reproduce the experimental Raman vibrational frequencies and intensities, we already calculated the minimum energy structures and Raman spectra for G and G radical species using DFT. B3LYP/6-311++G(d,p) and B3LYP/6-31G(d) are used for calculating the Raman spectrum for G, $G^{\bullet}(-H^+)$, $G^{\bullet+}$, and $(G^{\bullet+})'$. For radical cations, we used unrestricted molecular orbitals. In this case, the $\langle S^2 \rangle$ value was kept at around 0.76. We also considered the solvation effect with a polarized continuum model using an integral equation formalism (IEF-PCM). Thus, the dielectric solvation field of water was applied on the target molecule for the geometry optimization as well as for the vibration frequency calculations. Two Na^+ were added for balancing the total charge instead of putting two protons on the phosphate. In the case of G, the positions and relative intensities of the calculated Raman peaks were well-matched with experimental results except for the relative intensity of the Pyr ring mode localized at N3 at 1177 cm^{-1} and the C═O stretching frequency at >1650 cm^{-1} (Figure 1). The difference between the experimental and calculated C═O stretching frequencies at >1650 cm^{-1} was larger than that in other peaks. Using a larger basis set made the C═O frequency shift down, which resulted in better agreement with our experimental result. However, both basis sets failed to give a larger intensity of the Pyr ring mode localized at N3 at 1177 cm^{-1}.

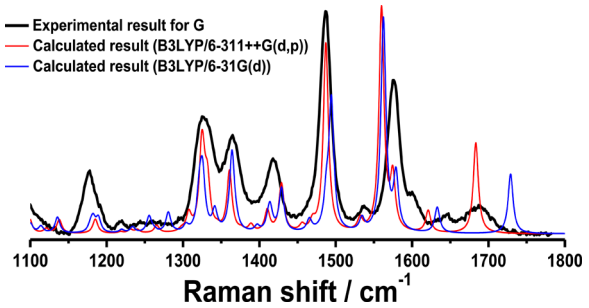

Figure 1. Experimental and theoretical Raman spectra of 5′-dGMP (scaling factor: 0.986 for 6-311++G(d,p) and 0.976 for 6-31G(d)).

On the other hand, the Raman bands measured for $(G^{\bullet+})'$ were slightly up-shifted relative to those of G except for the C═O stretching, which was followed by the appearance of a new Raman band at 1266 cm^{-1} (Figure 2). As shown in Figure 2, no calculated Raman spectra for $G^{\bullet}(-H^+)$, $G^{\bullet+}$, and $(G^{\bullet+})'$ could reproduce the experimental Raman vibrational frequencies and intensities. In particular, the calculated Raman spectra for $G^{\bullet}(-H^+)$, $G^{\bullet+}$, and $(G^{\bullet+})'$ still showed the C═O stretching at 1600−1750 cm^{-1}, which is consistent with those calculated by Sevilla et al. However, our experimental TR^3 spectra did not show any Raman band at 1600−1780 cm^{-1}, indicating that the C6—O stretching mode for G radical species moved into the low-frequency range (<1600 cm^{-1}). This experimental result means that the formation of G radical species resulted in a decrease in the C6═O bonding order.

To reproduce the experimental TR^3 spectrum around 1600 cm^{-1} using DFT calculations, a smaller scaling factor, 0.94, has to be applied to the calculated Raman spectra. The application of a smaller scaling factor leads to a wrong interpretation that

Received: January 22, 2016
Revised: February 29, 2016
Published: March 1, 2016

DOI: 10.1021/acs.jpcb.6b00713
J. Phys. Chem. B 2016, 120, 2987−2989

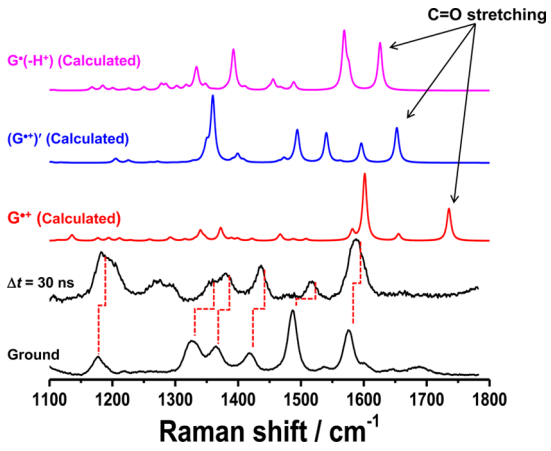

Figure 2. Steady-state Raman spectrum of 5′-dGMP (bottom line) and TR^3 spectrum observed at Δt = 30 ns after pulse radiolysis of 50 mM 5′-dGMP and the calculated Raman spectra for $G^{\bullet}(-H^+)$, $G^{\bullet+}$, and $(G^{\bullet+})'$ (scaling factor: 0.976). Raman spectra for G radical species were calculated with B3LYP/6-31G(d).

the Raman band at 1587 cm^{-1} must be interpreted as C6═O stretching down-shifted upon oxidation of G. Generally, it is well-known that the down-shift of the Raman band comes from the decrease in the bonding order. However, as mentioned above, the decrease in the C═O bonding order results in the C—O stretching at ∼1250 and ∼1510 cm^{-1}, corresponding to the C—O single bond and partial C┅O double bond, respectively. In this respect, the Raman band at 1587 cm^{-1} cannot be interpreted as C6═O stretching down-shifted upon oxidation of G. Considering the vibrational frequency and intensity of the Raman band at 1587 cm^{-1}, the Raman band at 1587 cm^{-1} is probably due to the Pyr ring mode which was contributed largely from the motion of N3. In addition, the Raman band at 1516 cm^{-1} is attributed to the Pyr ring CN stretching coupled with C8H deformation but not a partial C┅O double bond stretching. Consequently, we assigned the Raman band at 1266 cm^{-1} to a C—O single bond due to an unpaired electron localized on the oxygen (O6) of the Pyr ring, although we did not give direct evidence for the origin of the Raman band at 1266 cm^{-1}, as pointed out by Sevilla et al. It is accepted that the phenoxyl radical with a C—O single bond character shows a vibration mode at ∼1250 cm^{-1},[2,3] although the frequency for a C—O single bond is close to that for phenol calculated by Sevilla et al. (1270 cm^{-1}). Indeed, the C—O stretching with a single bond character in many organic molecules has been observed at 1200−1300 cm^{-1}.[4−6] For example, Tahara et al. reported that the C—O stretching frequency for T_1 benzophenone (BP) with a single bond character is 1222 cm^{-1}, whereas the corresponding value in S_0 BP is 1665 cm^{-1}.[6] These previous studies for Raman C—O stretching modes with a single bond character support our interpretation that the Raman band at 1266 cm^{-1} is due to a C—O single bond stretching due to an unpaired electron localized on the oxygen (O6) of the Pyr ring.

In addition, Sevilla et al. showed that, using the DFT calculation, the unpaired electron is fully delocalized as is typical for π-radicals. The DFT calculation is a very useful method to predict a variety of molecular properties, such as molecular structures, vibrational frequencies, ionization energies, electric and magnetic properties, reaction paths, etc., in the ground state. However, as mentioned above, there are still difficulties in using the DFT calculation to reproduce a molecular structure and Raman vibrational frequencies and intensities of transient radical species. To reproduce resonance Raman spectra, the effect of resonance should be considered, although inclusion of this effect is quite difficult. As mentioned above, the comparison of the experimental and theoretical Raman spectrum for G radical species shows a significant discrepancy. Thus, we tentatively interpreted the molecular structure of G radical species based on our experimental results and suggest that the unpaired electron in G radical species is localized on the oxygen of the Pyr ring, which results in the C—O stretching mode at 1266 cm^{-1}.

Finally, Sevilla et al. suggested that the protonation of $G^{\bullet}(-H^+)$ thermodynamically takes place at N1, but not N7. Our DFT calculations showed that $G^{\bullet+}$ is favored by 11.7 kcal/mol over $(G^{\bullet+})'$, which is consistent with the calculation result by Sevilla et al. In addition, our DFT calculations also revealed that $G^{\bullet+}$ is more stable than $G^{\bullet}(-H^+)$. These DFT calculations indicate that only the $G^{\bullet+}$ can exist under experimental conditions. However, the structure of $G^{\bullet}(-H^+)$ has been detected by many research groups.[7−10] Unfortunately, this discrepancy means that our DFT calculation cannot accurately predict the structure and energy of G radical species.

It is known that the pK_a of N1 in $G^{\bullet+}$ was experimentally determined to be 3.9.[7] However, the plot of the rate constant against the pH value demonstrates that the pK_a for the protonation of $G^{\bullet}(-H^+)$ may be higher than 6.0. This experimental result clearly indicates that the protonation of N1 can be ruled out. Furthermore, our experimental result (transient absorption spectral change) demonstrates that the deprotonation at N1 of $G^{\bullet+}$ rapidly occurs within 30 ns (3.3×10^7 s^{-1}). Considering the deprotonation rate ($k_d > 3.3 \times 10^7$ s^{-1}), the pK_a of 3.9 of N1, and the pH value of solutions (pH ∼ 7), the protonation rate constant k_p at N1 can be estimated to be about $\geq 2.6 \times 10^4$ s^{-1} under our experimental conditions. The small value for k_p implies that the reprotonation at N1 takes place in the time range of microseconds. From this point of view, in $G^{\bullet}(-H^+)$, N3 and N7 can be considered as a protonation site, but not N1. Indeed, Giese and McNaughton demonstrated that the proton affinity for protonation at N7 of G is calculated to be 945 kJ mol^{-1},[11] which is close to that reported by Greco et al. (951 ± 48 kJ mol^{-1}).[12] Giese and McNaughton also suggested that N7, and not N3, is the preferred protonation site in both aqueous solution and solid states. Steenken suggested that $G^{\bullet+}$ in neutral solutions is in equilibrium with $(G^{\bullet+})'$ (see Scheme II in ref 8). Tomasz et al. proposed that the isotope exchange at the C8 site of the imidazole (Im) ring requires the protonation at N7 as a first step at various pH values at 37 °C,[13] meaning that the N7 of the Im ring can be easily protonated under physiological conditions. Therefore, we suggest that the fast dynamics observed in the transient absorption measurement is due to the protonation at N7 of $G^{\bullet}(-H^+)$.

In summary, we are responding to the comment of Sevilla et al., which challenged the structure of G radical species and the reprotonation site of $G^{\bullet}(-H^+)$. During the review process of our previous study, we already considered the structure of G radical species and the reprotonation site of $G^{\bullet}(-H^+)$ using DFT calculations and then carefully compared the experimental and theoretical results. As shown in Figures 1 and 2, DFT calculations failed to reproduce the experimental Raman vibrational frequencies and intensities for G and G radical species. Calculations by Sevilla et al. also did not provide reasonable explanations for present Raman spectra. Thus, the

DOI: 10.1021/acs.jpcb.6b00713
J. Phys. Chem. B 2016, 120, 2987−2989

improvement of MO theory by inclusion of the resonance effect is essential. Now, we are investigating this point. Moreover, we did not obtain the experimental evidence for the protonation at N1 of $G^{\bullet}(-H^{+})$. Thus, we suggested the reprotonation at N7 of $G^{\bullet}(-H^{+})$ and the localization of the unpaired electron at O6 in G radical species. To confirm the structures of G radical species and C−O bond character, we will measure the TR^3 spectrum of ^{18}O isotope-substituted guanine in the near future. On the other hand, in our original paper, we suggested that the $(G^{\bullet+})'$ may act as a precursor for the formation of 8-oxoguanine radical (8-oxo-$G^{\bullet}$) by OH addition in aqueous solutions, which suggests the existence of 8-oxo-$G^{\bullet}$. We will investigate the formation of 8-oxo-$G^{\bullet}$ using ^{18}O isotope-substituted water.

AUTHOR INFORMATION

Corresponding Authors

*E-mail: jkchoi@ibs.re.kr.

*E-mail: majima@sanken.osaka-u.ac.jp.

Notes

The authors declare no competing financial interest.

ACKNOWLEDGMENTS

We are grateful to Dr. Doo-Sik Ahn for valuable discussions. We also thank the members of the Research Laboratory for Quantum Beam Science of ISIR, Osaka University, for running the linear accelerator. This work was partly supported by a Grant-in-Aid for Scientific Research (projects 25220806 and 25288035) from the Ministry of Education, Culture, Sports, Science and Technology (MEXT) of Japanese Government. This work was supported by IBS-R004-G2.

REFERENCES

(1) Choi, J.; Yang, C.; Fujitsuka, M.; Tojo, S.; Ihee, H.; Majima, T. Proton Transfer of Guanine Radical Cations Studied by Time-Resolved Resonance Raman Spectroscopy Combined with Pulse Radiolysis. *J. Phys. Chem. Lett.* **2015**, *6*, 5045−5050.

(2) Beck, S. M.; Brus, L. E. The Resonance Raman-Spectra of Aqueous Phenoxy and Phenoxy-D_5 Radicals. *J. Chem. Phys.* **1982**, *76*, 4700−4704.

(3) Mukherjee, A.; Mcglashen, M. L.; Spiro, T. G. Ultraviolet Resonance Raman-Spectroscopy and General Valence Force-Field Analysis of Phenolate and Phenoxyl Radical. *J. Phys. Chem.* **1995**, *99*, 4912−4917.

(4) Tahara, T.; Hamaguchi, H.; Tasumi, M. Transient Resonance Raman-Spectra of Benzophenone and Its Four Isotopic Analogs in the Lowest Excited Triplet-State. *J. Phys. Chem.* **1987**, *91*, 5875−5880.

(5) Nagano, Y.; Liu, J.-G.; Naruta, Y.; Ikoma, T.; Tero-Kubota, S.; Kitagawa, T. Characterization of the Phenoxyl Radical in Model Complexes for the CuB Site of Cytochrome *c* Oxidase: Steady-State and Transient Absorption Measurements, UV Resonance Raman Spectroscopy, EPR Spectroscopy, and DFT Calculations for M-BIAIP. *J. Am. Chem. Soc.* **2006**, *128*, 14560−14570.

(6) Tahara, T.; Hamaguchi, H.; Tasumi, M. UV-Excited Transient Raman-Spectra and the CO Stretching Frequencies of the Lowest Excited Triplet-State of Benzophenone. *Chem. Phys. Lett.* **1988**, *152*, 135−139.

(7) Kobayashi, K.; Tagawa, S. Direct Observation of Guanine Radical Cation Deprotonation in Duplex DNA using Pulse Radiolysis. *J. Am. Chem. Soc.* **2003**, *125*, 10213−10218.

(8) Steenken, S. Purine-Bases, Nucleosides, and Nucleotides: Aqueous-Solution Redox Chemistry and Transformation Reactions of Their Radical Cations and e^{-} and OH Adducts. *Chem. Rev.* **1989**, *89*, 503−520.

(9) Morozova, O. B.; Saprygina, N. N.; Fedorova, O. S.; Yurkovskaya, A. V. Deprotonation of Transient Guanosyl Cation Radical Catalyzed by Buffer in Aqueous Solution: TR-CIDNP Study. *Appl. Magn. Reson.* **2011**, *41*, 239−250.

(10) Candeias, L. P.; Steenken, S. Structure and Acid-Base Properties of One-Electron-Oxidized Deoxyguanosine, Guanosine, and 1-Methylguanosine. *J. Am. Chem. Soc.* **1989**, *111*, 1094−1099.

(11) Giese, B.; McNaughton, D. Density Functional Theoretical (DFT) and Surface-Enhanced Raman Spectroscopic Study of Guanine and Its Alkylated Derivatives: Part 1. DFT Calculations on Neutral, Protonated and Deprotonated Guanine. *Phys. Chem. Chem. Phys.* **2002**, *4*, 5161−5170.

(12) Greco, F.; Liguori, A.; Sindona, G.; Uccella, N. Gas-Phase Proton Affinity of Deoxyribonucleosides and Related Nucleobases by Fast-Atom-Bombardment Tandem Mass-Spectrometry. *J. Am. Chem. Soc.* **1990**, *112*, 9092−9096.

(13) Tomasz, M.; Olson, J.; Mercado, C. M. Mechanism of the Isotopic Exchange of the C-8 Hydrogen of Purines in Nucleosides and in Deoxyribonucleic Acid. *Biochemistry* **1972**, *11*, 1235−1241.

DOI: 10.1021/acs.jpcb.6b00713
J. Phys. Chem. B 2016, 120, 2987−2989